Desalination and Water Treatment
www.deswater.com
doi: 10.5004/dwt.2020.25351

184 (2020) 39–50
April

Effect of shape of condensing cover on yield of passive and fully covered PVT active solar still

A.K. Mishra[a], Md. Meraj[b,*], G.N. Tiwari[c,d], A. Ahmad[a], M.E. Khan[b]

[a]*Electrical Engineering Department, Faculty of Engineering and Technology, AFU, Faridabad, India, Tel. +919811534676; email: mishra_anil62@yahoo.com (A.K. Mishra), azizjmi98@gmail.com (A. Ahmad)*
[b]*Mechanical Engineering Department, Faculty of Engineering and Technology, JMI, New Delhi, India, Tel. +919897965833; email: md.meraj1221@gmail.com (Md. Meraj), mekhan@jmi.ac.in (M.E. Khan)*
[c]*Professor (Research), SRM University, Deva Road, Lucknow (UP), India*
[d]*Bag Energy Research Society, 11B, Gyan Khand IV, Indrapuram, Ghaziabad, UP, India, Tel. +919318466512; email: gntiwari@ces.iitd.ernet.in (G.N. Tiwari)*

Received 9 July 2019; Accepted 11 December 2019

ABSTRACT

In this communication, an analytical expressions of water temperature, condensing cover temperature, yield and electrical power of self-sustained photovoltaic thermal-active solar distillation system has been derived in terms of design and climatic parameters. Effect of inclination of single slope and conical shape of condensing cover on an overall thermal and exergy of the proposed system have also been studied. On the basis of numerical computation, the following conclusions have been drawn: (i) The yield is optimum with conical shape of condensing cover with inclination of 60° at water depth of 0.01 m and mass flow rate of 0.01 kg/s; (ii) The yield decreases with the increase in water depth at larger mass flow rate >0.01 kg/s as per our expectation and vice-versa for lower mass flow rate.

Keywords: Solar still; Purification of water; Rectangular and conical condensing cover

1. Introduction

Water is the most precious gift of nature. It is essential for existence and survival. There is a huge shortage of safe drinking water posing a great threat for survival to life on the planet. Water scarcity arises due to a high rise in population, rapid industrial development and large scale farming activities to produce enough food grains [1]. Large scale deforestation and climate change are also responsible for water stress. The health of billions of people around the world is affected due to drinking unsafe water. Consuming contaminated water causes water-borne diseases and is responsible for the untimely death of a large number of people. Another important reason for water crisis is due to the attitude of sheer carelessness and negligence by the majority of urban dwellers. Before modernization and advent of technology people were able to get water for their usage from drawing it from well, river fountain etc. They cultivated the habit of using water sparingly utilizing every drop of water optimally. For minimizing water stress it is must learn to conserve, preserve, recycle, recharge water table by water harvesting.

Solar stills are a viable solution to produce safe drinking water in far remote locations, where it is not feasible to transport water, facing drought-like situation, not having power connectivity or facing frequent power outages. Most of the available desalination technologies are powered by conventional energy produced by the combustion of fossil fuels. Fossil fuels are depleting at an alarming rate and detrimental to the environment and health [2]. Solar still has a

* Corresponding author.

bright future because of the simple technology used for producing potable water, easy to maintain and operate, environmental-friendly and economically viable [3]. Solar distillation is a process of producing safe drinking water from saline/contaminated water using thermal energy from solar radiation. Heat energy received is directly utilized to evaporate contaminated water kept inside an airtight chamber known as a solar still.

Solar stills are classified into two categories, one is passive solar still and the other one is active solar still. Tiwari and Sahota [4] have carried out a detailed study of passive and self-sustained active solar still working under forced mode to compare their energy and economic efficiencies. In the case of a passive solar still, basin water is directly heated by solar radiation. A lot of design of passive solar still have been studied and presented by several authors. Malik et al. [5] have evaluated and reported passive solar distillation up to 1982. Tiwari and Lawrence [6] have updated the work done on passive solar still including active solar still. Tiwari and Tiwari [7] have investigated and presented the influences of various parameters on the productivity of passive solar still. Dwivedi and Tiwari [8] have presented energy and exergy analysis of single as well as double slope passive solar still. Tiwari and Sahota [9] have written a book on advanced solar distillations in which authors have described functioning and thermal modeling of passive and active solar stills.

In the case of active solar still additional thermal energy is fed by external mode [10] to enhance the temperature difference between evaporating and conducting surface. The active solar still is classified as fossil fuel-based (conventional flat plate collector (FPC) integrated) and solar energy-based photovoltaic thermal (PVT integrated) under force mode of operation. In fossil fuel-based solar still, fossil fuel is used to power (electricity) the pump. Various researchers have reported on solar distillation integrated with FPC/concentrator. Rai and Tiwari [11] have worked on active solar still the first time in forced mode. They have reported that the temperature of brine solutions is influenced by mass flow rate, the quantum of solar radiation received and types and the quality of heat storage materials. Lawrence and Tiwari [12] have carried out a theoretical evaluation of solar distillation in thermosyphon mode. Zaki et al. [13] have presented an experimental investigation coupled with concentrator assisted solar still. Tiwari et al. [14] have developed the thermal model for the active solar still integrated with different types of solar collectors and compared experimental results with theoretical values. Boubekri et al. [15] have conducted a numerical computation on active solar still integrated with PVT-SWH in addition to internal and external reflectors. Singh et al. [16] reported on active solar distillation with partially covered photovoltaic FPC. Mishra et al. [17] have investigated performance evaluation of active solar still in natural mode. Recently, Manokar et al. [18] have presented a comprehensive review of the solar still integrated with PVT technologies. Naroei et al. [19] have performed an experimental and numerical analysis on the performance of stepped active solar still connected with PVT water collector. Elbar and Hassan [20] have demonstrated experimentation on the performance of active solar still coupled with photovoltaic module as a reflector. They have done their work on the opaque photovoltaic module. Nayi and Modi [21] have illustrated a comprehensive review of the recent techniques for solar still performance improvement and the latest development and challenges in the research of pyramid solar still. Further, Selvaraj and Natarajan [22] have discussed a detailed review of the various factor influencing the productivity and performances of solar stills. They have concluded that besides the conventional methods, there are few methods, namely, absorbing plate materials, floating plates, wick materials, energy-storing materials, the addition of fins, reflectors, vacuum tubes, etc. can be used for the improvement of the productivity of still. Panchal et al. [23] have demonstrated experimentation on various techniques to enhance the yield of tubular solar still. None of the above authors have reported the effect of shape of condensing cover in active solar still under forced mode. In this research paper, the shape of the condensing cover has been taken as conical for different inclinations to increase the area of condensing cover. Basin area in all the three cases, that is, for conventional single slope passive solar still, active solar still integrated with PVT-FPC and conical active solar still coupled with PVT-FPC remain the same that is 1 m^2. With an increase in the area of condensing cover, the hourly yield will increase but water temperature will reduce. In the present study, fully covered semi-transparent PVT-FPC has been considered unlike others.

2. System description

Fig. 1 represents an active conventional solar still coupled with fully covered semi-transparent PVT-FPC. The conventional solar still is made of fibre reinforced plastic which serves as an insulator to minimize heat loss from the basin. Its top cover is made of transparent glass in rectangular shape through which direct solar radiation (direct gain) reaches in the rectangular shape basin having an effective area A_b = 1 m^2 (as shown in Fig. 1). In order to receive optimum heat energy orientation of solar still is most important. The orientation of a single slope is kept south facing for better performance. For optimum yield, the inclination of condensing cover is taken equal to 15° for the summer point of view. The basin liner and side walls are painted black to absorb maximum heat reaching the basin. In this case, water is heated directly (direct gain) and also indirectly using the PVT-FPC. The main objective of integrating PVT-FPC with conventional passive solar still is to feed the hot water into a basin and electric power generation which is used to run the motor for circulation of basin water in a closed-loop through the collector. This arrangement will enhance the temperature gradient between the water surface and the inner condensing cover. Passive solar still operates at a lower temperature range but active solar still operates at a higher temperature range. With a gain in temperature, the rate of evaporation increases which results in increased yield from solar still as compared to that of passive solar still. Further, to study the effect of the shape of condensing covers, a PVT-FPC integrated active solar still having conical shape condensing cover and a circular basin area of an effective area A_b = 1 m^2 (as shown in Fig. 2) has been considered. In this case, to see the effect of inclination on the performance, the inclination of conical condensing cover is

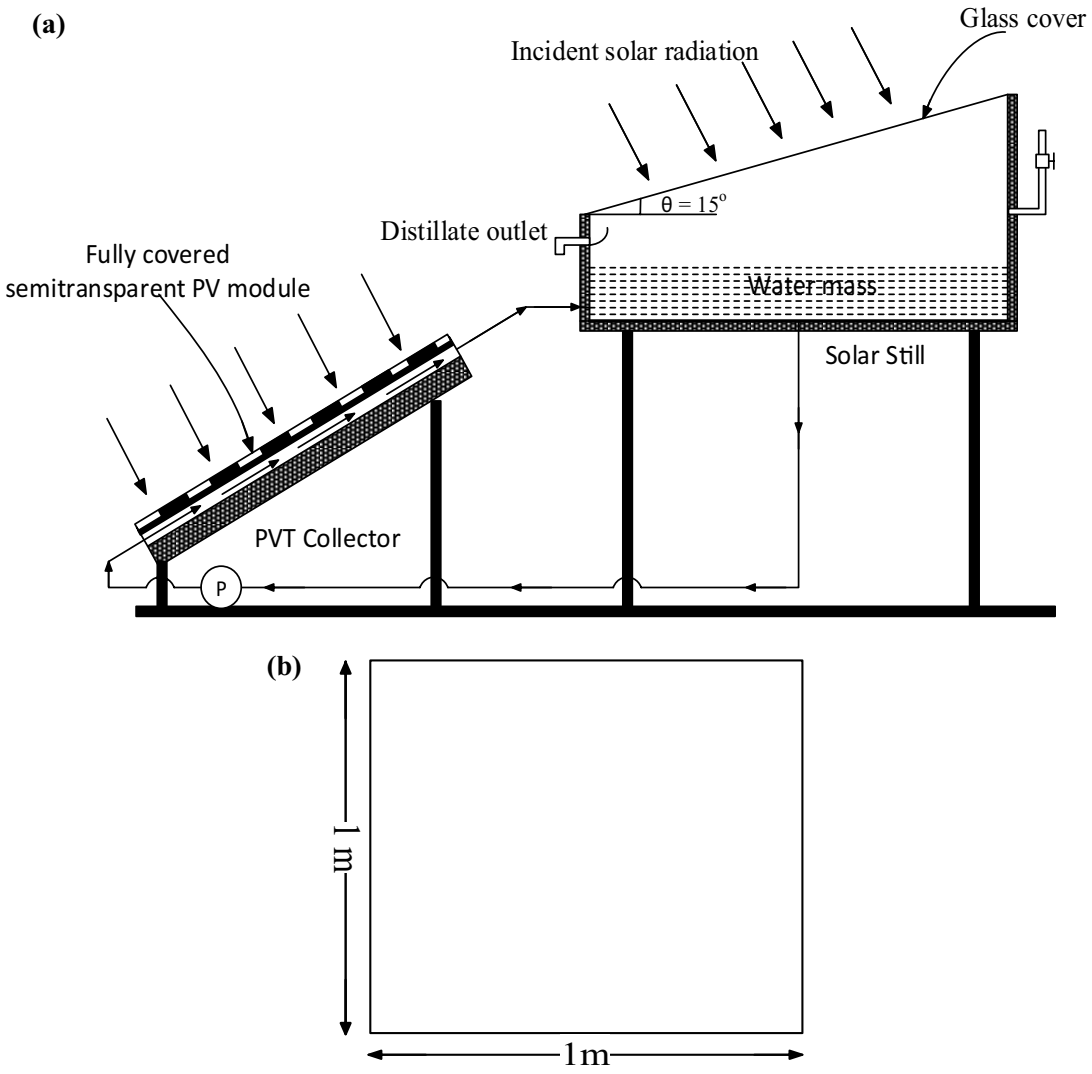

Fig. 1. (a) Schematic representation of active conventional solar still having rectangular basin shape of an effective area A_b = 1 m^2 coupled with fully covered semi-transparent PVT-FPC and (b) rectangular shape of a basin.

changed from 15° to 60° (referring to Fig. 2). For comparative analysis, the basin area of all the three configurations has been kept same, that is, 1 m^2 under same operating conditions and following condensing cover shape has been considered:

- Rectangular condensing cover for passive and active solar still.
- Conical condensing cover for active solar still.

3. Thermal modeling

For the purpose of simplification of the numerical simulation of the proposed model, the following assumptions are needed that are given as bellows:

- Whole process in the proposed system is considered under the quasi-steady state conditions.
- Heat capacities of the materials used in the design of the proposed model are neglected.
- One-dimensional heat flow has been considered for the present simulation.
- Ohmic losses between the solar cells of PVT-FPC collectors are neglected.
- There is no stratification of temperature between layers of fluid.
- Vapor leakage proof system is considered.
- Pressure losses in the pipe flow are neglected.

3.1. Photovoltaic thermal-flat plate collector (PVT-FPC)

3.1.1. Energy balance for solar cells of PVT-FPC

Following Tiwari et al. [24,25], the energy balance for the PVT-FPC integrated with the solar still is presented as given below:

$$\alpha_c \tau_g \beta_c I_c A_m = U_{t,\mathrm{ca}} \left(T_c - T_a\right) A_m + U_{t,\mathrm{cp}} \left(T_c - T_p\right) A_m + \eta_c \tau_g \beta_c I_c A_m \quad (1)$$

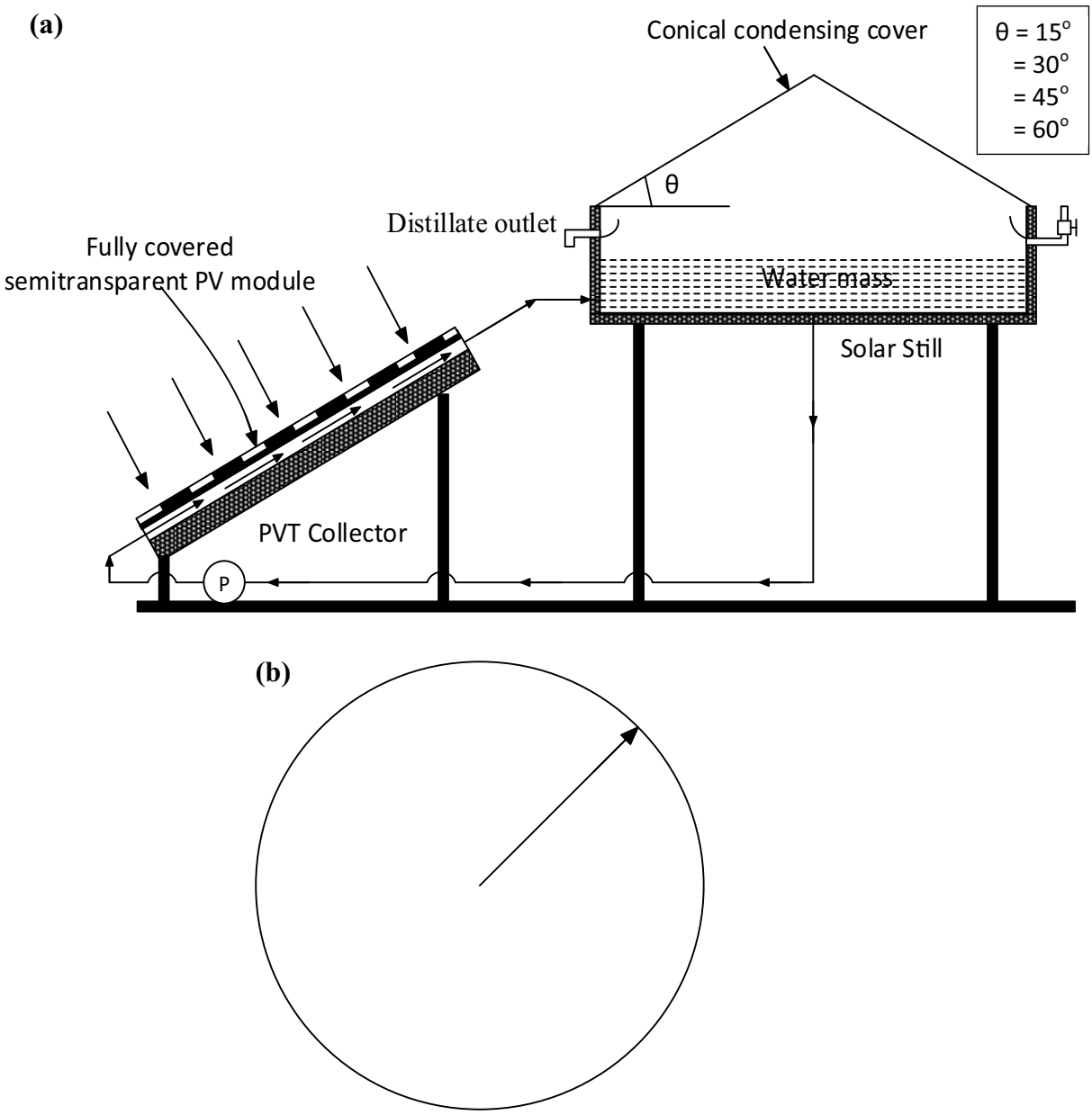

Fig. 2. (a) Schematic representation of PVT-FPC integrated active solar still having conical shape condensing cover and circular basin area of an effective area A_b = 1 m² and (b) circular shape of a basin (proposed model).

[Incident radiation on PVT-FPC] = [Heat loss from the solar cell to ambient from top surface] + [Heat transferred from solar cell to absorber surface through glass] + [Electrical power generated by the photovoltaic module of PVT-FPC].

From Eq. (1), the corresponding solar cell temperature of photovoltaic module of the collector can be obtained as follows:

$$T_c = \frac{(\alpha\tau)_{1,\text{eff}} I_c + U_{t,\text{ca}} T_a + U_{t,\text{cp}} T_p}{U_{t,\text{ca}} + U_{t,\text{cp}}} \quad (2)$$

3.1.2. Energy balance for absorber plate of PVT-FPC

Similarly, the energy balance for the blackened tube in plate absorber having high thermal conductivity below the photovoltaic module of the collector is shown below:

$$\alpha_c \tau_g^2 (1-\beta_c) I_c A_m + U_{t,\text{cp}} \left(T_c - T_p\right) A_m = F' h_{\text{pf}} \left(T_p - T_f\right) A_m + U_{t,\text{pa}} \left(T_p - T_a\right) A_m \quad (3)$$

[Solar radiation available on the absorber plate through the non-packing area photovoltaic module of collector]

+ [Rate of heat transferred from solar cell to absorber plate due to temperature difference] = [Rate of heat carried away by the fluid flowing through the tubes of absorber plate] + [Heat loses from the absorber plate to the ambient].

With the help of Eqs. (2) and (3), the absorber plate temperature can be obtained as given below:

$$T_p = \frac{\left[\left(\alpha\tau\right)_{2,\text{eff}} + \text{PF}_1\left(\alpha\tau\right)_{1,\text{eff}}\right]_c + U_{L2}T_a + F'h_{\text{pf}}T_f}{U_{L2} + F'h_{\text{pf}}} \tag{4}$$

3.1.3. Energy balance for the flowing fluid

Further, the rate of thermal energy carried away by the flowing fluid through the tubes of the absorber plate below the semi-transparent photovoltaic module of the PVT-FPC can be expressed as follows:

$$\dot{m}_f C_f \frac{dT_f}{dx}dx = F'h_{\text{pf}}\left(T_p - T_f\right)bdx \tag{5}$$

On substitution of Eq. (4) into the above equation, the above expressions can the rewritten as:

$$\dot{m}_f C_f \frac{dT_f}{dx}dx = F'\left[\text{PF}_2\left(\alpha\tau\right)_{m,\text{eff}} I_c - U_{\text{Lm}}\left(T_f - T_a\right)\right]bdx \tag{6}$$

Since in the present modeling, the PVT-FPC is connected with the solar still (referred to Fig. 2), thus Eq. (6) can be solved by using initial condition, $T_f|_{x=0} = T_{\text{fi}} = T_w$, the solution can be obtained as follows:

$$T_f = \left[\frac{\text{PF}_2\left(\alpha\tau\right)_{m,\text{eff}} I_c}{U_{\text{Lm}}} + T_a\right]\left[1 - \exp\left\{\frac{-F'U_{\text{Lm}}bx}{\dot{m}_f C_f}\right\}\right] + T_w \exp\left\{\frac{-F'U_{\text{Lm}}bx}{\dot{m}_f C_f}\right\} \tag{7}$$

Further, the temperature of the fluid at the outlet of the PVT-FPC, which is fed to the solar still as shown in Fig. 2 can be obtained as follows:

$$T_{f_0} = T_f|_{x=L_{\text{rm}}} \tag{8}$$

or,

$$T_{f0} = \left[\frac{\text{PF}_2\left(\alpha\tau\right)_{m,\text{eff}} I_c}{U_{\text{Lm1}}} + T_a\right]\left[1 - \exp\left\{\frac{-F'U_{\text{Lm}}bL_{\text{rm}}}{\dot{m}_f C_f}\right\}\right] + T_w \exp\left\{\frac{-F'U_{\text{Lm}}bL_{\text{rm}}}{\dot{m}_f C_f}\right\} \tag{9}$$

or,

$$T_{f0} = \left[\frac{\text{PF}_2\left(\alpha\tau\right)_{m,\text{eff}} I_c}{U_{\text{Lm1}}} + T_a\right]\left[1 - \exp\left\{\frac{-F'_{U_{\text{Lm}}}A_m}{\dot{m}_f C_f}\right\}\right] + T_w \exp\left\{\frac{-F'_{U_{\text{Lm}}}A_m}{\dot{m}_f C_f}\right\} \tag{10}$$

Later on, the rate of useful heat gain at the outlet of PVT-FPC can be estimated as follows:

$$\dot{Q}_u = \dot{m}_f C_f\left(T_{f_0} - T_w\right) \tag{11}$$

On substitution of Eq. (10) into Eq. (11), the expression for $\dot{Q}_u$ can be represented as follows:

$$\dot{Q}_u = A_m F_{\text{Rm}}\left[\text{PF}_2\left(\alpha\tau\right)_{m,\text{eff}} I_c - U_{\text{Lm}}\left(T_w - T_a\right)\right] \tag{12}$$

Numerical values for the terms PF_1, PF_2, $(\alpha\tau)_{1,\text{eff}}$, $(\alpha\tau)_{2,\text{eff}}$, $(\alpha\tau)_{m,\text{eff}}$, F_{Rm}, etc. have been given in Table 1.

Following Schott [26] and Evans [27], the temperature-dependent electrical efficiency of the solar cell of photovoltaic module of the collector is given as follows:

$$\eta_c = \eta_0\left[1 - \beta_0\left(T_c - T_0\right)\right] \tag{13}$$

Further, on substitution of Eqs. (2), (4) and (7) in the above equation, the expression for η_c for the PVT-FPC can be written as follows:

$$\eta_c = \frac{\eta_0\left[1 - \beta_0\left[\frac{1}{U_{t,\text{ca}} + U_{t,\text{cp}}}\left[I_c\left[\alpha_c\tau_g\beta_c + \frac{U_{t,\text{cp}}}{U_{L2} + F'h_{\text{pf}}}\left\{\left(\alpha\tau\right)_{2,\text{eff}} + \text{PF}_1\alpha_c\tau_g\beta_c\right\} + \frac{U_{t,\text{cp}}F'h_{\text{pf}}}{2\dot{m}_f C_f\left(U_{L2} + F'h_{\text{pf}}\right)}\left\{\text{PF}_2\left(\alpha\tau\right)_{2,\text{eff}} + \text{PF}_2\text{PF}_1\alpha_c\tau_g\beta_c\right\}A_m F_{\text{Rm}}\right] + T_a\left[U_{t,\text{ca}} + \frac{U_{t,\text{cp}}U_{L2}}{U_{L2} + F'h_{\text{pf}}} + \frac{U_{t,\text{cp}}F'h_{\text{pf}}}{2\dot{m}_f C_f\left(U_{L2} + F'h_{\text{pf}}\right)}\left\{A_m F_{\text{Rm}}U_{\text{Lm}}\right\}\right] + T_w\left[\frac{U_{t,\text{cp}}F'h_{\text{pf}}\left(1 + K_m\right)}{2\left(U_{L2} + F'h_{\text{pf}}\right)}\right]\right] - T_0\right]\right]}{\left[1 - \frac{\eta_0\beta_0 I_c}{U_{t,\text{ca}} + U_{t,\text{cp}}}\left[\tau_g\beta_c + \frac{U_{t,\text{cp}}}{U_{L2} + F'h_{\text{pf}}}\text{PF}_1\tau_g\beta_c + \frac{U_{t,\text{cp}}F'h_{\text{pf}}}{2\dot{m}_f C_f\left(U_{L2} + F'h_{\text{pf}}\right)}\text{PF}_2\text{PF}_1\tau_g\beta_c A_m F_{\text{Rm}}\right]\right]} \tag{14}$$

Table 1
Design parameters used in numerical computation

A_m = 2.1 m^2	$U_{t,\mathrm{pa}}$ = 4.8 W/m^2 K
A_b = 1 m^2	h_{pf} = 100 W/m^2
F' = 0.9680	h_i = 5.7 W/m^2
F_{Rm} = 0.8050	h'_i = 5.8 W/m^2
K_g = 0.816 W/m K	h_0 = 9.5 W/m^2
L_g = 0.003 m	h_w = 100 W/m^2
K_i = 0.166 W/m K	α'_{eff} = 0.7600
L_i = 0.100 m	$(\alpha\tau)_{\mathrm{eff}}$ = 0.5241
K_m = 0.6832 W/m K	$(\alpha\tau)_{1,\mathrm{eff}}$ = 0.6375
K_p = 6 W/m K	$(\alpha\tau)_{2,\mathrm{eff}}$ = 0.0794
L_p = 0.002 m	$(\alpha\tau)_{m,\mathrm{eff}}$ = 0.3205
L_i = 0.100 m	α_c = 0.9
PF_1 = 0.3782	α'_b = 0.5861
PF_2 = 0.9512	α'_g = 0.0095
U = 10.75 W/m^2 K	α'_w = 0.1787
$\mathrm{UA}_{\mathrm{eff}}$ = 10.75 W/m^2 K	α_p = 0.8
U_{L1} = 3.47 W/m^2 K	β_0 = 0.0045
U_{L2} = 8.27 W/m^2 K	β_c = 0.89–0.25
U_{Lm} = 7.87 W/m^2 K	τ_g = 0.95
$U_{t,\mathrm{ca}}$ = 9.17 W/m^2 K	C_f = 4,200 J/kg K
$U_{t,\mathrm{cp}}$ = 5.58 W/m^2 K	

Now, using Eq. (14), the electrical efficiency and electrical power output of module of PVT-FPC can be evaluated as follows:

$$\eta_m = \tau_g \beta_c \eta_c \tag{15}$$

and,

$$E_{\mathrm{el}} = \eta_m A_m I_c \tag{16}$$

respectively.

3.2. Energy balance for solar still

3.2.1. Energy balance equation for condensing cover of still

Following Tiwari [10], energy balance equation for glass cover of solar still can be written as follows:

$$\alpha'_g I_{\mathrm{co}} A_{\mathrm{co}} + h_{1w}\left(T_w - T_{\mathrm{co}}\right)A_b = h_2\left(T_{\mathrm{co}} - T_a\right)A_{\mathrm{co}} \tag{17}$$

[Incident solar radiation over condensing cover + equivalent heat transfers from water to glass] = [Heat loss from condensing cover to ambient by convection].

From Eq. (17), the equation for the temperature of condensing cover is obtained as follows:

$$T_{\mathrm{co}} = \frac{\alpha'_g I_{\mathrm{co}} A_{1,\mathrm{eff}} + h_{1w} T_w + h_2 A_{1,\mathrm{eff}} T_{\mathrm{amb}}}{\left(h_{1w} + h_2 A_{1,\mathrm{eff}}\right)} \tag{18}$$

where $A_{1,\mathrm{eff}} = \frac{A_{\mathrm{co}}}{A_b} A_{\mathrm{co}}$ is are of condensing cover and A_b is the area of basin of the solar still.

Further, on solving Eq. (17) for, one can obtain the expression as follow:

$$h_{1w}\left(T_w - T_{\mathrm{co}}\right) = U_t\left(T_w - T_a\right) - \alpha'_g I_{\mathrm{co}} H \tag{19}$$

where, $U_t = \frac{h_{1w} h_2 A_{1,\mathrm{eff}}}{h_{1w} + h_2 A_{1,\mathrm{eff}}}$ and $H = \frac{h_{1w} A_{1,\mathrm{eff}}}{h_{1w} + h_2 A_{1,\mathrm{eff}}}$.

3.2.2. Energy balance equation for basin liner of still

The net energy as absorbed by the basin can be presented as the sum of the heat transferred to basin water and heat loss through bottom insulation.

$$\alpha'_b I_{\mathrm{co}} A_b = h_3\left(T_b - T_w\right)A_b + h_b\left(T_b - T_a\right)A_b \tag{20}$$

From Eq. (20), one can obtain the expression for a temperature of the basin as follows:

$$T_b = \frac{\alpha'_b I_{\mathrm{co}} + T_w h_{1w} + h_b T_a}{h_3 + h_b} \tag{21}$$

Later on, solving Eq. (20), one can obtain the expression for $h_3\left(T_b - T_w\right)$ as follow:

$$h_3\left(T_b - T_w\right) = \alpha'_g I_{\mathrm{co}} H_1 - U_{\mathrm{wa}}\left(T_w - T_a\right) \tag{22}$$

where, $H_1 = \frac{h_3}{h_3 + h_b}$ and $U_{\mathrm{wa}} = \frac{h_3 h_b}{h_3 + h_b}$.

3.2.3. Energy balance equation for water of still

The energy balance for the water mass of active solar still integrated with PVT-CPC has been represented as follows:

$$\dot{Q}_u + \alpha'_b I_{\mathrm{co}} A_b + h_3\left(T_b - T_w\right)A_b = M_w C_w \frac{dT_w}{dT} + h_{1w}\left(T_w - T_g\right)A_b \tag{23}$$

where $\dot{Q}_u$ is the useful heat gain (Eq. 12) fed to the solar till by PVT-FPC.

Further, using Eqs. (12), (19) and (22), one can write the resultant equation as given below:

$$\frac{dT_w}{dt} + aT_w = f\left(t\right) \tag{24}$$

where $a = \frac{1}{M_w C_w}\left(U + UA_{\mathrm{eff}}\right)$

and

$$f\left(t\right) = \frac{1}{M_w C_w}\left[\left(\left(\alpha\tau\right)_{\mathrm{eff}} + \alpha'_{\mathrm{eff}}\right)I_{\mathrm{co}} + \left(U + UA_{\mathrm{eff}}\right)T_a\right] \tag{25}$$

The numerical values for $(\alpha\tau)_{\mathrm{eff}}$, $(\alpha\tau)'_{\mathrm{eff}}$, U and $\mathrm{UA}_{\mathrm{eff}}$ have been given in Table 1.

On solving the differential equation, the temperature of water in solar still is obtained as

$$T_w = \frac{\overline{f(t)}}{a}\left[1-\exp\left(-a\Delta t\right)\right] + T_{w0}\exp\left(-a\Delta t\right) \quad (26)$$

where T_{w0} is temperature of basin water at t = 0 and T_{w0} is temperature of basin water at $t = 0$ and $\overline{f(t)}$ is the average value of $f(t)$ for time interval 0 to t.

The rate of heat losses in the form of evaporation in the solar still and hourly yield of the proposed model can be evaluated as follows:

$$\dot{q}_{ew} = h_{ew}\left(T_w - T_{co}\right)\frac{\mathrm{W}}{\mathrm{m}^2} \quad (27)$$

$$m_{ew} = \frac{h_{ew}\left(T_w - T_{co}\right)}{L}\times 3{,}600\ \mathrm{kg/m^2h} \quad (28)$$

where h_{ew} is the evaporative loss coefficient and L is the latent heat of vaporization of water.

Further, the hourly overall energy gain of the proposed active solar still can be obtained as given below:

$$E_{ovll} = \dot{q}_{ew}A_{co} + \frac{E_{el}}{\xi_p} \quad (29)$$

The daily overall energy gain of the system can be obtained from the above expression as follows:

$$\sum_{t=1}^{n}E_{ovll} = \sum_{t=1}^{n}\dot{q}_{ew}A_{co} + \frac{\sum_{t=1}^{n}E_{el}}{\xi_p} \quad (30)$$

where n is the number of working hours of the system and 'ξ_p' is the conversion power factor of coal-based power plant. 'ξ_p' is taken as 0.38 for good quality coal-based power plant, otherwise, it would be lower [28].

Later on, the hourly overall exergy gain of the proposed active solar still can be obtained as given below:

$$Ex_{ovll} = h_{ew}A_{co}\left[\left(T_w - T_{co}\right) - \left(T_a - 273\right)\ln\left(\frac{T_w + 273}{T_{co} + 273}\right)\right] + E_{el} \quad (31)$$

Similarly, the daily overall exergy gain of the system can be obtained from the above expression as follows:

$$\sum_{t=1}^{n}Ex_{ovll} = \sum_{t=1}^{n}h_{ew}A_{co}\left[\left(T_w - T_{co}\right) - \left(T_a - 273\right)\ln\left(\frac{T_w + 273}{T_{co} + 273}\right)\right] + \sum_{t=1}^{n}E_{el} \quad (32)$$

4. Methodology

The following methodology has been adopted for the analysis of the proposed design

- *Step 1*: Climatic data's such as solar radiation and ambient temperature on a horizontal surface for a typical day in the month of March for New Delhi have been taken from Indian Meteorological Department (IMD), Pune, India. The solar radiation harnessed by PVT collector and solar still has been calculated by using Liu and Jordan [29]. The hourly variations of solar radiation and ambient temperature have been shown in Fig. 3.
- *Step 2*: Corresponding to above climatic data and the design parameters (as illustrated in Table 1), the outlet fluid temperature of a collector, condensing cover temperature and water mass of soar still have been computed by using Eqs. (10), (18) and (26) respectively.
- *Step 3*: With the help of above calculated parameters, Eqs. (12) and (16) have been used to obtain the rate of useful thermal energy gain and electrical power output respectively.
- *Step 4*: With the help of above calculated data, Eq. (28) has been used to compute the hourly yield of the proposed design.
- *Step 5*: Further, Eq. (29) and (30) have been used to evaluate the hourly and daily overall energy gain, while Eq. (31) and (32) have been used to estimate the hourly and daily overall exergy gain.

5. Results and discussion

Eqs. (10), (18) and (26) have been computed to evaluate the hourly variation of outlet fluid temperature (T_{fo}) of PVT-FPC, condensing cover (T_{co}) and water mass temperature (T_w) of PVT-FPC integrated active solar still having conical shape condensing cover at inclination of 15° (as shown in Fig. 2). The numerical computation has been done at a mass flow rate of 0.01 kg/s and a water mass of 100 kg. The results have been represented in Fig. 4 along with ambient temperature for a typical day of March month taken from IMD. It can be seen from the figure that the outlet fluid temperature of collector and water mass temperature of still are almost the same from 8:00 to 17:00 due to maximum thermal energy input to the solar still through PVT-FPC at a lower mass flow rate. It can also be seen that the temperature difference between the maximum value of water mass and the corresponding condensing cover temperature is 12.8°C at 15:00 while the difference between the maximum value of condensing cover and corresponding ambient temperature is 13.4°C at 17:00.

Fig. 5 represents the hourly variation of the yield (Eq. (28)) of passive conventional solar still, active conventional solar still integrated with PVT-FPC and PVT-FPC integrated active solar still having conical condensing cover at different inclination (i.e. θ = 15°, 30°, 45°, and 60°). It can be observed from the figure that the yield of PVT-FPC integrated active solar still with conical condensing cover at an inclination of θ = 60°, mass flow rate of 0.01 kg/s and basin water mass of 100 kg is highest throughout among all other configuration due to more available condensing surface area. It can also be seen from the graph that the peak value of yield of proposed active solar still having conical condensing cover at an inclination of θ = 60° is 0.1993 and 0.0536 kg/m^{2}h higher than the corresponding value of passive conventional and active conventional solar still.

Further, the effect of packing factor on the daily yield, electrical energy output, overall energy and exergy gain of PVT-FPC integrated active solar still having conical

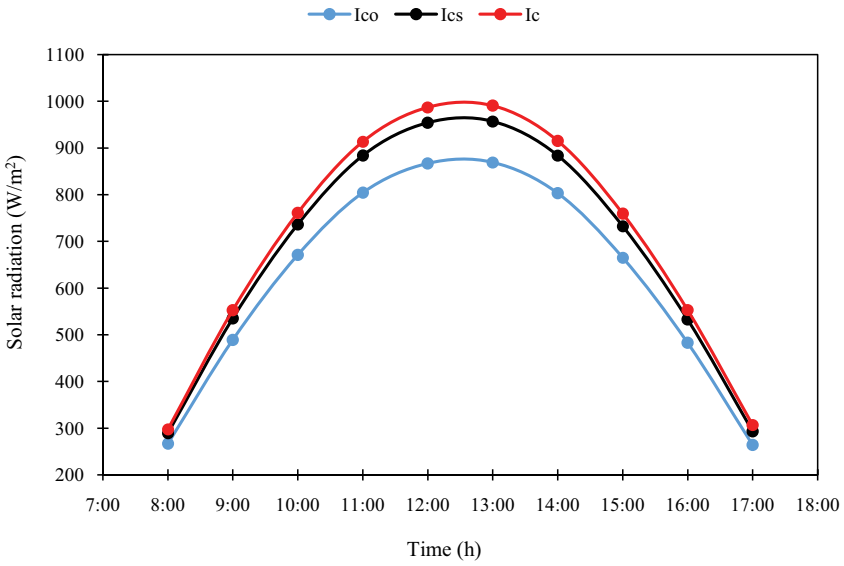

Fig. 3. Hourly variation of solar radiation on the conical solar still, conventional solar still and PVT collector.

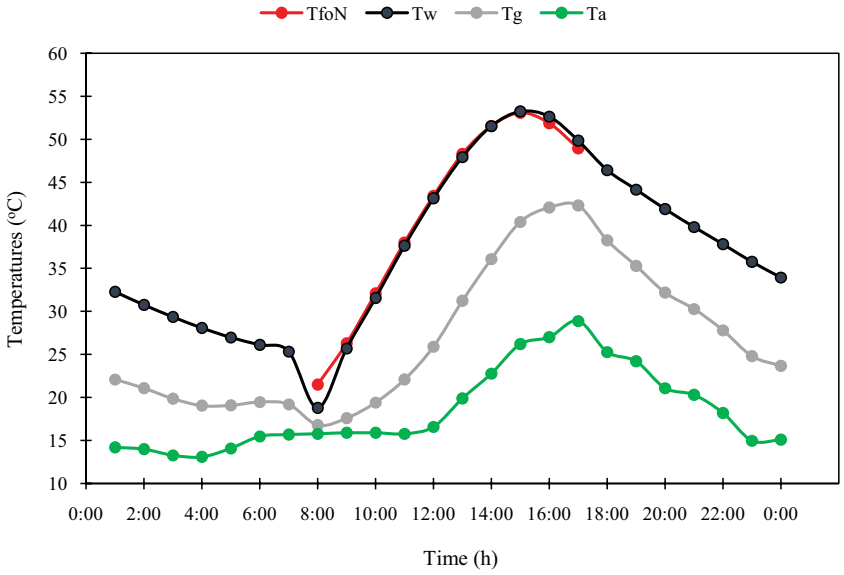

Fig. 4. Hourly variation of outlet fluid temperature, water mass temperature, condensing cover temperature and ambient temperature.

condensing cover at θ = 60°, mass flow rate of 0.01 kg/s and basin water mass of 100 kg (i.e. 0.01 m depth) have been shown in Figs. 6 and 7. From the figures, it is found that the daily yield and overall energy gain of the proposed design are increasing with the decrease in the packing factor of the module of PVT-FPC due to the increase in a non-packing area which results in increasing the direct thermal gain through the PVT-FPC. However, it can also be observed from the graphs that the daily electrical energy output and overall exergy gain is decreasing on the decrement of packing factor because of a decrease in the number of solar cells of a module which results in lower electrical power output. Hence, it is concluded from the figures that the lower packing factor β_c = 0.25 of the proposed solar still has optimum yield (9.7 kg/d) with a sufficient amount of electrical energy (0.483 kWh/d) to make the system self-sustained.

Later on, the effect of basin water mass on the daily yield and electrical energy output of the proposed active solar still having conical condensing cover inclination of θ = 60°, packing factor β_c = 0.25 for different mass flow rate (i.e. $\dot{m}_f$ = 0.01 and 0.07 kg/s) have been illustrated in Fig. 8. It can be seen from Fig. 8a that at small mass flow rate (i.e. 0.01 kg/s), the yield of the proposed model increases with the increase of the basin water mass. It is due to the reason for maximum thermal energy input at a lower mass flow rate and an increase in thermal capacity on the increase of water mass. From Fig. 8b it can be found that at higher mass flow rate (i.e. 0.07 kg/s) yield decreases with the increase of basin

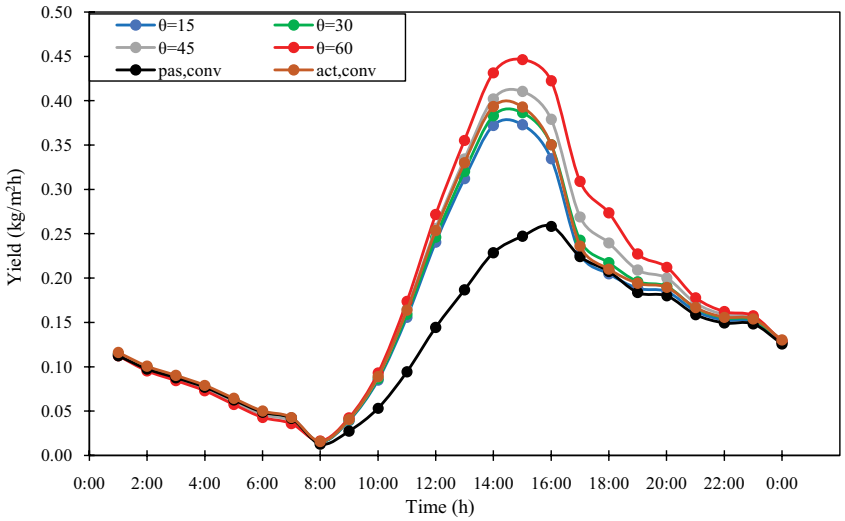

Fig. 5. Hourly variation of yield of passive conventional solar still, active conventional solar still and active solar still having conical condensing surface with different inclination.

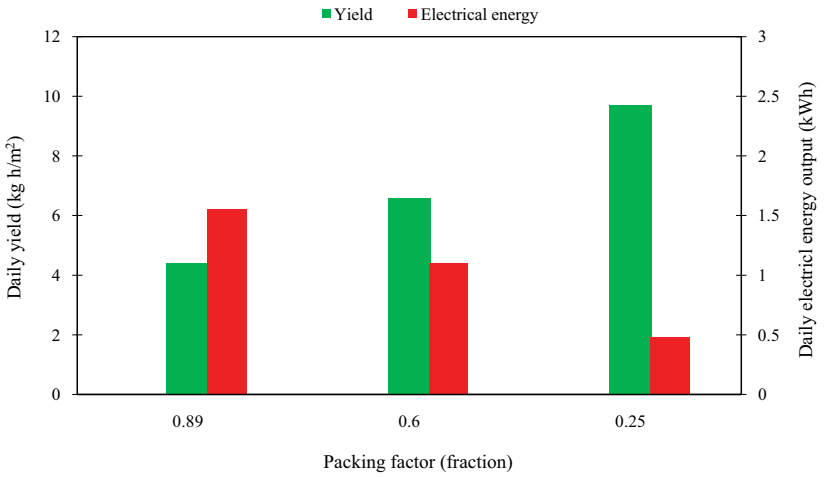

Fig. 6. Effect of packing factor on the yield and electrical energy output of active solar still having conical condensing surface at θ = 60°.

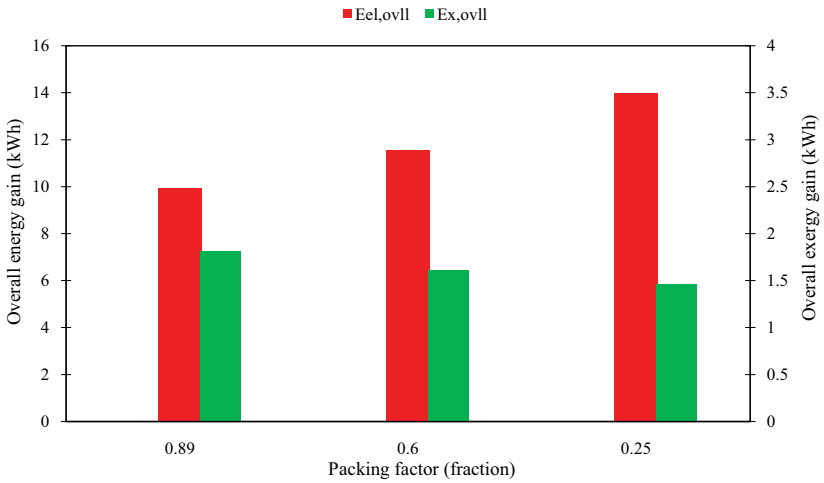

Fig. 7. Effect of packing factor on overall energy and exergy gain of active solar still having conical condensing surface at θ = 60°.

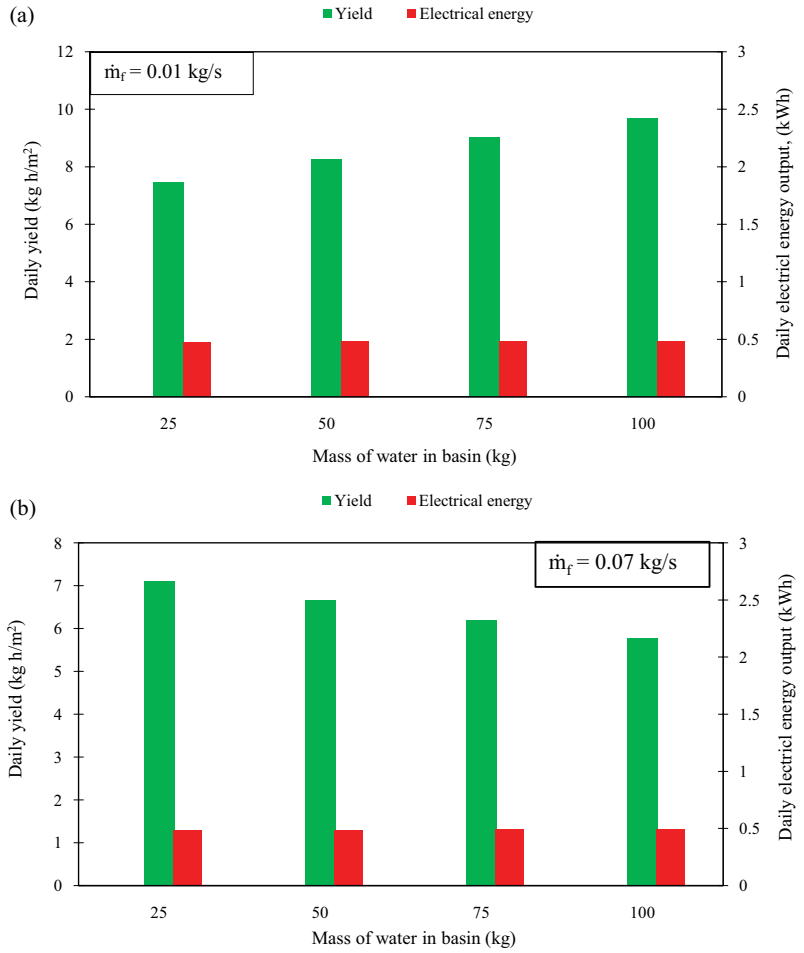

Fig. 8. Effect of water mass on the yield and electrical energy output at of active solar still having conical condensing surface (θ = 60°) at a mass flow rate of (a) 0.01 and (b) 0.07 kg/s.

water mass as per our expectation. It can also be seen from this figure that the daily electrical output of the proposed system is nearly the same due to the fact of the same number of solar cells present in the module of PVT-FPC having fixed packing factor (β_c = 0.25).

6. Conclusions and recommendation

On the basis of present studies, the following conclusions have been drawn:

- The yield of PVT-FPC integrated active solar still with conical condensing cover at an inclination of 60° is optimum with respect to other cases under the study.
- From an energy and exergy point of view, the proposed design of active solar still is most suitable.
- At small mass flow rate, that is, $\dot{m}_f$ = 0.01 kg/s, the yield increases from 7.4 to 9.7 kg h/m² with the increase of water depth from 0.025 to 0.10 m (Fig. 8a).
- At a higher mass flow rate (>0.07 kg/s), the yield decreases with the increase of water depth (Fig. 8b). This is in accordance with the results reported by many researchers [9].
- The proposed thermal model for PVT-FPC integrated conical solar still should be validated by the experiment. We are unable to validate the model due to financial problems in our institute.

Symbols

A_b	—	Area of basin of a solar still, m²
A_{co}	—	Area of condensing cover of a solar still, m²
A_m	—	Area of module of PVT-FPC, m²
C_f	—	Specific heat of fluid, J/kg K
$\dot{E}_{el}$	—	Electrical power output, W or kWh/m²
E_{ovll}	—	Overall energy gain, W or kWh/m²
Ex_{ovll}	—	Overall exergy gain, W or kWh/m²
F'	—	Collector efficiency factor
H	—	Penalty factor
h_i	—	Heat transfer coefficient for space between the glazing and absorption plate, W/m² K
h'_i	—	Heat transfer coefficient from the bottom of PVT to ambient, W/m² K
h_0	—	Heat transfer coefficient from the top, W/m² K
h_{pf}	—	Heat transfer coefficient from absorber plate to fluid, W/m² K
I	—	Solar radiation/intensity, W/m²

K_g — Thermal conductivity of glass, W/m K
K_i — Thermal conductivity of insulation, W/m K
K_p — Thermal conductivity of absorption plate, W/m K
L_g — Thickness of glass cover, m
L_i — Thickness of insulation, m
L_p — Thickness of absorption plate, m
$\dot{m}_{ew}$ — Hourly yield for proposed still, kg/h
$\dot{m}_f$ — Mass flow rate of fluid, kg/s
PF_1 — Penalty factor due to glass covers of photovoltaic module
PF_2 — Penalty factor due to absorption plate below photovoltaic module
$\dot{Q}_u$ — The rate of useful heat gain, W or kWh/m^2
$\dot{q}_{ew}$ — The rate of evaporative heat loss in the solar still, W/m^2
T_a — Ambient temperature, °C
T_b — Temperature of basin liner of a solar still, °C
T_c — Solar cell temperature, °C
T_{co} — Temperature of condensing cover of solar still, °C
T_{fi} — Fluid inlet temperature at entry of PVT-FPC, °C
T_{fo} — Fluid outlet temperature at end of PVT-FPC, °C
T_w — Temperature of water in solar still, °C
T_p — Absorption plate temperature, °C
T_0 — Reference cell temperature for optimum cell efficiency, that is, 25°C
U_{Lm} — Overall heat loss coefficient from module to ambient, W/m^2 K
U_t — Top heat loss coefficient, W/m^2 K
$U_{t,ca}$ — Overall heat loss coefficient from cell to ambient, W/m^2 K
$U_{t,cp}$ — Overall heat loss coefficient from cell to plate, W/m^2 K
$U_{t,pa}$ — Overall heat loss coefficient from plate to ambient, W/m^2 K
U_{wa} — Heat loss coefficient from water to ambient, W/m^2 K
V — Air velocity, m/s

Greek letters

α — Absorptivity
β — Packing factor
β_0 — Temperature coefficient of efficiency
θ — Inclination of condensing cover in degree
ρ — Reflectivity
τ — Transmittivity
η — Efficiency
$(\alpha\tau)_{eff}$ — Product of effective absorptivity and transmittivity

Subscripts

a — Ambient
c — Solar cell/collector
eff — Effective
f — Fluid
fi — Inlet fluid
fo — Outlet fluid
co — Condensing cover
cs — Conventional still
m — Module
ovll — Overall
p — Plate
w — Water

References

[1] P.S. Goh, A.F. Ismail, N. Hilal, Nano-enabled membrane technology, sustainable and revolutionary solutions for membrane desalination, Desalination, 380 (2016) 100–104.
[2] H.E.S. Fath, Solar distillation a promising alternative for water provision with free energy, simple technology, and clean environment, Desalination, 116 (1998) 45–56.
[3] H.E.S. Fath, H.M. Hosny, Thermal performance of single-sloped basin still with an inherent built-in additional condenser, Desalination, 142 (2002) 19–27.
[4] G.N. Tiwari, L. Sahota, Review on energy and economic efficiencies of passive and active solar distillation systems, Desalination, 401 (2017) 151–179.
[5] M.A.S. Malik, G.N. Tiwari, A. Kumar, M.S. Sodha, Solar Distillation, 1st ed., Pergamon Press, Oxford, UK, 1982.
[6] G.N. Tiwari, S.A. Lawrence, Heat and mass transfer relationship for solar still, Energy Convers. Manage., 31 (1992) 201–203.
[7] A.K. Tiwari, G.N. Tiwari, Thermal modeling based on solar fraction and experimental study of the annual and seasonal performance of a single slope passive solar still: the effect of water depths, Desalination, 207 (2007) 184–204.
[8] V.K. Dwivedi, G.N. Tiwari, Annual energy and exergy analysis of single and double slope passive solar stills, Trends Appl. Sci., 3 (2008) 225–241.
[9] G.N. Tiwari, L. Sahota, Advanced Solar-Distillation Systems: Basics Principles, Thermal Modeling and Its Applications, Springer Publication, Singapore, 2017.
[10] G.N. Tiwari, Solar Energy: Fundamentals, Design, Modeling and Applications, Narosa Publishing House, New Delhi, India, 2002.
[11] S.N. Rai, G.N. Tiwari, Single basin solar still coupled with flat plate collector, Energy Convers. Manage., 23 (1983) 145–149.
[12] S.A. Lawrence, G.N. Tiwari, Theoretical evaluation of solar distillation and natural circulation with heat exchanger, Energy Convers. Manage., 30 (1992) 205–213.
[13] G.M. Zaki, A. Al-Turki, M. Al-Falani, Experimental investigation on concentrator assisted solar stills, Sol. Energy, 11 (1992) 193–199.
[14] G.N. Tiwari, V. Dimri, U. Singh, A. Chel, B. Sarkar, Comparative thermal performance evaluation of an active solar distillation system, Int. J. Energy Res., 31 (2007) 1465–1482.
[15] M. Boubekri, A. Chaker, A. Cheknane, Modeling and simulation of the continuous production of an improved solar still coupled with a photovoltaic/thermal solar water heater system, Desalination, 331 (2013) 6–15.
[16] D.B. Singh, J.K. Yadav, V.K. Dwivedi, S. Kumar, G.N. Tiwari, I.M. Al-Helal, Experimental studies of active solar studies integrated with two hybrid PVT collectors, Sol. Energy, 130 (2016) 207–233.
[17] K.N. Mishra, M. Meraj, A.K. Tiwari, G.N. Tiwari, Performance evaluation of PVT-CPC integrated solar still under natural circulation, Desal. Wat. Treat., 156 (2019) 117–125.
[18] A.M. Manokar, D.P. Winston, A.E. Kabeel, S.A. El-Agouz, R. Sathyamurthy, T. Arunkumar, T. Madhu, A. Ahsan, Integrated PV/T solar still - a mini-review, Desalination, 435 (2018) 259–267.
[19] M. Naroei, F. Sarhaddi, F. Sobhnamayan, Efficiency of a photovoltaic thermal stepped solar still: experimental and numerical analysis, Desalination, 441 (2018) 87–95.
[20] A.R.A. Elbar, H. Hassan, Experimental investigation on the impact of thermal energy storage on the solar still performance coupled with PV module via new integration, Sol. Energy, 184 (2019) 584–593.
[21] K.H. Nayi, K.V. Modi, Pyramid solar still: a comprehensive review, Renewable Sustainable Energy Rev., 81 (2018) 136–148.
[22] K. Selvaraj, A. Natarajan, Factors influencing the performance and productivity of solar stills-a review, Desalination, 435 (2018) 181–187.

[23] H. Panchal, K.K. Sadasivuni, M. Israr, N. Thakar, Various techniques to enhance distillate output of tubular solar still: a review, Groundwater Sustainable Dev., 9 (2019) 100268.
[24] G.N. Tiwari, M. Meraj, M.E. Khan, R.K. Mishra, V. Garg, Improved Hottel-Whillier-Bliss equation for N-photovoltaic thermal-compound parabolic concentrator (N-PVT-CPC) collector, Sol. Energy, 166 (2018) 203–212.
[25] G.N. Tiwari, M. Meraj, M.E. Khan, Exergy analysis of N-photovoltaic thermal-compound parabolic concentrator (N-PVT-CPC) collector for constant collection temperature for vapor absorption refrigeration (VAR) system, Sol. Energy, 173 (2018) 1032–1042.
[26] T. Schott, Operational Temperatures of PV Modules-a Theoretical and Experimental Approach, Proc. 6th PV Solar Energy Conference, 1985, pp. 392–396.
[27] D.L. Evans, Simplified method for predicting photovoltaic array output, Sol. Energy, 27 (1981) 555–560.
[28] B.J. Huang, T.H. Lin, W.C. Hung, F.S. Sun, Performance evaluation of solar photovoltaic/thermal systems, Sol. Energy, 70 (2001) 443–448.
[29] B.Y.H. Liu, R.C. Jordan, The interrelationship and characteristic distribution of direct, diffuse and total solar radiation, Sol. Energy, 4 (1960) 1–19.